Hindawi
Wireless Communications and Mobile Computing
Volume 2017, Article ID 9171068, 13 pages
https://doi.org/10.1155/2017/9171068

WILEY | Hindawi

Research Article

Iterative Multiuser Equalization for Subconnected Hybrid mmWave Massive MIMO Architecture

R. Magueta,[1] V. Mendes,[1] D. Castanheira,[1] A. Silva,[1] R. Dinis,[2] and A. Gameiro[1]

[1]*Instituto de Telecomunicações (IT) and DETI, Universidade de Aveiro, Aveiro, Portugal*
[2]*Instituto de Telecomunicações (IT) and Faculdade de Ciências e Tecnologia, Universidade Nova de Lisboa, Caparica, Portugal*

Correspondence should be addressed to R. Magueta; rlm@ua.pt

Received 1 August 2017; Accepted 3 December 2017; Published 20 December 2017

Academic Editor: Patrick Seeling

Millimeter waves and massive MIMO are a promising combination to achieve the multi-Gb/s required by future 5G wireless systems. However, fully digital architectures are not feasible due to hardware limitations, which means that there is a need to design signal processing techniques for hybrid analog-digital architectures. In this manuscript, we propose a hybrid iterative block multiuser equalizer for subconnected millimeter wave massive MIMO systems. The low complexity user-terminals employ pure-analog random precoders, each with a single RF chain. For the base station, a subconnected hybrid analog-digital equalizer is designed to remove multiuser interference. The hybrid equalizer is optimized using the average bit-error-rate as a metric. Due to the coupling between the RF chains in the optimization problem, the computation of the optimal solutions is too complex. To address this problem, we compute the analog part of the equalizer sequentially over the RF chains using a dictionary built from the array response vectors. The proposed subconnected hybrid iterative multiuser equalizer is compared with a recently proposed fully connected approach. The results show that the performance of the proposed scheme is close to the fully connected hybrid approach counterpart after just a few iterations.

1. Introduction

A new generation of cellular network (fifth generation, 5G) is coming, and some innovative technologies are needed to ensure better performance and quality of service (QoS). Two enabling technologies have been considered to meet the QoS requirements for future wireless communication, massive MIMO (mMIMO), and millimeter wave (mmWave) communications [1]. By using mmWave bands, several tens of GHz of bandwidth become available for wireless systems [2], while the mMIMO allows the continued increasing demand of higher data rates for future wireless networks [3]. Comparing the mMIMO with conventional MIMO approaches, the mMIMO can scale up the conventional MIMO by orders of magnitude [4]. A survey on mMIMO, also identified as large-scale MIMO, with channel modelling, applications scenarios, and physical/networking techniques can be seen in [5]. The use of mmWave with mMIMO is very promising, because smaller wavelength compared to conventional communication systems allows the same volume to pack more antennas [6], which means that the terminals can support a large number of antennas.

The mmWave mMIMO combination can be used to exploit new efficient spatial processing techniques, such as beamforming/precoding and spatial multiplexing, at both transmitter and/or receiver terminals [7]. These techniques are different than those used for sub-6 GHz bands due to limitations in hardware [8]. In these systems, it is not practical to have one fully dedicated radio frequency (RF) chain by antenna [9] as in sub-6 GHz conventional MIMO systems [10] due to the power consumption and the high cost of mmWave mixed-signal components. Another issue is the mmWave propagation characteristics, which are quite different from sub-6 GHz because the mmWave channels are not so rich in multipath propagation effects [11, 12], which should be taken into consideration in the techniques design for these systems. To overcome the limitation of the RFs chains number, purely analog beamforming can use phase shifters [8], with some schemes proposed in [13, 14], where statistical channel knowledge is used through phase shifters,

to optimally adjust the arrays response in space, applying a beam steering solution.

The performance of the pure-analog techniques is limited by constraints on the amplitudes of phase shifters and due to the phases of the ones quantized. Therefore, analog beamforming is usually limited to single-stream transmission [15]. These limitations are overcome by doing some signal processing at an analog level and the rest at the digital level. These architectures are called hybrid analog/digital architectures and have been addressed in [15, 16]. Precoding and/or combining/equalization designs for single-user systems have been addressed for fully connected hybrid architectures in [17–19]. In these architectures, each of the RF chains is connected to all receive-and-transmit antennas. In [17], a hybrid spatially sparse precoding/combining approach was designed for mmWave mMIMO systems. The spatial structure of mmWave channels was used to transform the single-user multistream precoding and combining scheme into a sparse reconstruction problem. In [18], joint turbo-like beamforming was designed to compute transmit/receiving analog beamforming coefficients; however the digital processing part was not considered. In [19], codebook design approaches were addressed for single-stream transmissions through an analog beamforming structure. For multiuser systems, some beamforming approaches have been proposed for fully connected hybrid architectures [20–22]. The authors of [20] proposed uplink receiving beamforming where they assume only single antenna user-terminals (UTs), and at both stages analog and digital ones dealt with multiuser interference. Reference [21] proposed for the downlink a limited feedback analog/digital two-stage precoding and combining algorithm. Transmit/receiving analog beamforming are jointly computed in the first stage to maximize the power of the desired signal, and then the interference is explicitly mitigated using conventional linear zero-forcing (ZF) precoding in the second stage, that is, in the digital domain. An efficient hybrid iterative block space-time multiuser equalizer was proposed in [22]. This equalizer was designed based on the iterative block decision feedback equalization (IB-DFE) principle [23]. IB-DFE was originally proposed in [24]. It does not need the feedback loop of the channel decoder output, and it can be considered as a low complexity turbo equalizer. IB-DFE has been extended to several scenarios, like diversity scenarios and conventional and cooperative MIMO systems, among many others [25–30].

In addition to the fully connected architectures, there are subconnected architectures that allow us to reduce the number of phase shifters from NN^{RF} to N, when compared with fully connected counterparts, where N and N^{RF} are the number of antennas and the number of RF chains [31]. Thus, the power consumption used to excite and to compensate the insertion loss of phase shifters is reduced, and the computational complexity is also lower [31]. There are two types of subconnected architectures, dynamic and fixed [32]. In the dynamic subconnected case, each RF chain can dynamically connect to a different set of antennas, and in the fixed subconnected one, each RF chain is always physically connected to the same set of antennas. Precoding schemes for dynamic subconnected hybrid architectures have been proposed in [32, 33]. Reference [32] uses a relaxation of the mutual information maximization problem to design a technique that adapts the subarray structure according to the channel covariance matrix for frequency selective channels. The authors of [33] proposed a two-step algorithm for single-user narrowband systems that iteratively optimizes the hybrid precoder for spectral efficiency maximization, obtaining an extra data stream via the index of the active antenna set without any extra RF chain. Fixed subconnected hybrid architectures were addressed in [34–37]. In [34], precoder and combiner schemes for narrowband single-user systems are proposed, where a two-layer optimization method jointly exploiting the interference alignment and fractional programming was employed. First, the analog precoder and combiner are optimized via the alternating-direction optimization method, and then the digital precoder and combiner are optimized based on an effective channel matrix. The authors of [35] designed a precoder and a combiner for a wideband single-user system where the overall spectral efficiency is maximized considering a power budget constraint for each subcarrier. The works in [36, 37] are focused on multiuser downlink systems. In [36], the total achievable rate optimization problem with nonconvex constraints is decomposed to a series of sub-rate optimization problems for each subantenna array, and then an algorithm is implemented to perform a successive interference cancelation-based hybrid precoding. Precoding and combining schemes are performed in [37] for downlink, where virtual path selection maximizes the channel gain of the analog effective channel, and then a zero-forcing precoding in the digital domain is applied to mitigate the interference.

In this manuscript, we propose an efficient hybrid iterative block multiuser equalizer for subconnected mmWave mMIMO systems. The limitation that each RF chain is only physically connected to a subset of antennas makes the design of the proposed subconnected hybrid iterative multiuser equalizer harder than for the fully connected based approaches. To the best of our knowledge, iterative block detection designed for subconnected mmWave mMIMO architectures has not been addressed in the literature. We propose low complexity UTs without access to the Channel State Information (CSI), using a single RF chain and pure-analog random precoding. A time encoder/precoder is applied to guarantee that the transmit signal and thus the noise plus interference at the receiver side are Gaussian distributed. This not only simplifies the receiver optimization problem but also increases the diversity effects on the mmWave mMIMO system. The designed subconnected hybrid equalizer is optimized by using the average bit-error-rate (BER) as a metric. We compute the analog part of the equalizer sequentially over the RF chains using a dictionary built by the array response vectors. Finally, we show that the BER performance of the proposed subconnected hybrid iterative multiuser equalizer tends to the BER performance of a fully connected hybrid equalizer as the number of iterations increases.

This paper is organized as follows. Section 2 presents the subconnected hybrid multiuser mmWave mMIMO system

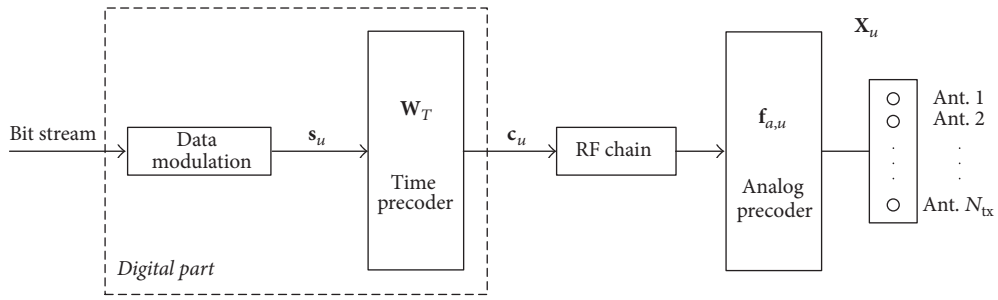

Figure 1: User-terminal u block diagram.

model. Section 3 begins with the description of a channel model for mmWave mMIMO systems, followed by the description of user-terminals (UT) and finally the design of the proposed subconnected hybrid iterative multiuser equalizer. Section 4 shows some BER performance results, and in Section 5, major conclusions are presented.

Notations. Matrices are denoted in boldface capital letters and column vectors in boldface lowercase letters. The operations $\text{tr}(\cdot)$, $(\cdot)^*$, $(\cdot)^T$, and $(\cdot)^H$ represent the trace, the conjugate, the transpose, and the Hermitian transpose of a matrix. $\text{sign}(a)$ is the operator that represents the sign of a real number a and $\text{sign}(c) = \text{sign}(\Re(c)) + j\,\text{sign}(\Im(c))$ if c is a complex number. It can also be employed elementwise to matrices. The functions $\Re(c)$ and $\Im(c)$ represent the real part and imaginary part of c. The functions $\text{diag}(\mathbf{a})$ and $\text{diag}(\mathbf{A})$, where $\mathbf{a}$ is a vector and $\mathbf{A}$ is a square matrix, correspond to a diagonal matrix where the entries of diagonal are equal to $\mathbf{a}$ and to a vector equal to the diagonal entries of $\mathbf{A}$. The element of row j and column l of matrix $\mathbf{B}$ is denoted by $\mathbf{B}(j,l)$. The identity matrix $N \times N$ is $\mathbf{I}_N$.

2. System Characterization

In this section, we describe the channel model, the UTs, and the receiver signals for the mmWave mMIMO system. We consider a multiuser system with U users, each one with N_{tx} transmit antennas, that sends one data stream per time slot to the base station with N_{rx} receiving antennas.

2.1. Channel Model. We consider a T-sized block fading channel, that is, a channel that remains constant during a block but varies independently between blocks. The channel follows the clustered sparse mmWave channel model discussed in [17] where $\mathbf{H}_u \in \mathbb{C}^{N_{\text{rx}} \times N_{\text{tx}}}$ is the channel matrix, which contributes the sum of N_{cl} clusters, each one with the contribution of N_{ray} propagation paths. The channel matrix may be expressed to the uth user as

$$\mathbf{H}_u = \gamma \sum_{j,l} \alpha_{jl,u} \Lambda_{\text{rx},u}\left(\phi_{jl}^{\text{rx},u}, \theta_{jl}^{\text{rx},u}\right) \Lambda_{\text{tx},u}\left(\phi_{jl}^{\text{tx},u}, \theta_{jl}^{\text{tx},u}\right) \times \mathbf{a}_{\text{rx},u}\left(\phi_{jl}^{\text{rx},u}, \theta_{jl}^{\text{rx},u}\right) \mathbf{a}_{\text{tx},u}\left(\phi_{jl}^{\text{tx},u}, \theta_{jl}^{\text{tx},u}\right)^H. \quad (1)$$

$\gamma = \sqrt{(N_{\text{tx}}N_{\text{rx}})/(N_{\text{cl}}N_{\text{ray}})}$ is a normalization factor, and $\alpha_{jl,u}$ is the complex gain of the lth ray in the jth scattering cluster. The functions $\Lambda_{\text{rx},u}(\phi_{jl}^{\text{rx},u}, \theta_{jl}^{\text{rx},u})$ and $\Lambda_{\text{tx},u}(\phi_{jl}^{\text{tx},u}, \theta_{jl}^{\text{tx},u})$ represent transmit and receiving antenna element gain for $\phi_{jl}^{\text{rx},u}(\theta_{jl}^{\text{rx},u})$ and $\phi_{jl}^{\text{tx},u}(\theta_{jl}^{\text{tx},u})$, that is, the azimuth (elevation) angles of arrival and departure. The vectors $\mathbf{a}_{\text{rx},u}(\phi_{jl}^{\text{rx},u}, \theta_{jl}^{\text{rx},u})$ and $\mathbf{a}_{\text{tx},u}(\phi_{jl}^{\text{tx},u}, \theta_{jl}^{\text{tx},u})$ represent the normalized receiving and transmit array response vectors for the corresponding angles. Reference [17] addressed the random distributions used to generate the path gains and the angles of channel, such that $\mathbb{E}[\|\mathbf{H}_u\|_F^2] = N_{\text{rx}}N_{\text{tx}}$.

2.2. User-Terminal Model Description. We assume that each user has only a single RF chain and sends only one data stream per time slot over the N_{tx} transmit antennas, as shown in Figure 1. We also consider that the UTs have no access to CSI, simplifying the overall system design. The analog precoder of uth UT at the instant t is mathematically modelled by $\mathbf{f}_{a,u,t} \in \mathbb{C}^{N_{\text{tx}}}$ and is physically realized using a vector of analog phase shifters, where all elements of vector $\mathbf{f}_{a,u,t}$ have equal norm ($|\mathbf{f}_{a,u,t}(l)|^2 = N_{\text{tx}}^{-1}$). Therefore, the analog precoder vector of the uth UT at the instant t is generated randomly according to

$$\mathbf{f}_{a,u,t} = \left[e^{j2\pi\phi_n^{u,t}}\right]_{1\le n\le N_{\text{tx}}, 1\le t\le T}, \quad (2)$$

where $\phi_n^{u,t}$ with $n \in \{1,\ldots,N_{\text{tx}}\}$, $t \in \{1,\ldots,T\}$ and $u \in \{1,\ldots,U\}$ are i.i.d. uniform random variables such that $\phi_n^{u,t} \in [0,1]$.

To guarantee that the transmit signal and then the noise plus interference are Gaussian distributed at the receiver side, the transmit signal $\mathbf{X}_u = [\mathbf{x}_{u,1},\ldots,\mathbf{x}_{u,T}]$ is built by using a space-time block code (STBC). A Discrete Fourier Transform (DFT) performs the time and the analog precoder performs the space encoding. The STBC simplifies receiver optimization and increases the diversity of the mmWave mMIMO system. Mathematically, the operation is expressed by

$$\mathbf{x}_{u,t} = \mathbf{f}_{a,u,t} c_{t,u}, \quad (3)$$

$$\mathbf{c}_u^T = \mathbf{s}_u^T \mathbf{W}_T, \quad (4)$$

where $\mathbf{W}_T \in \mathbb{C}^{T\times T}$ denotes a T-point DFT matrix and $\mathbf{c}_u = [c_{t,u}]_{1\le t\le T}$ is the time encoded version of $\mathbf{s}_u = [s_{t,u}]_{1\le t\le T} \in \mathbb{C}^T$. $s_{t,u}, t \in \{1,\ldots,T\}$ designates a complex data symbol

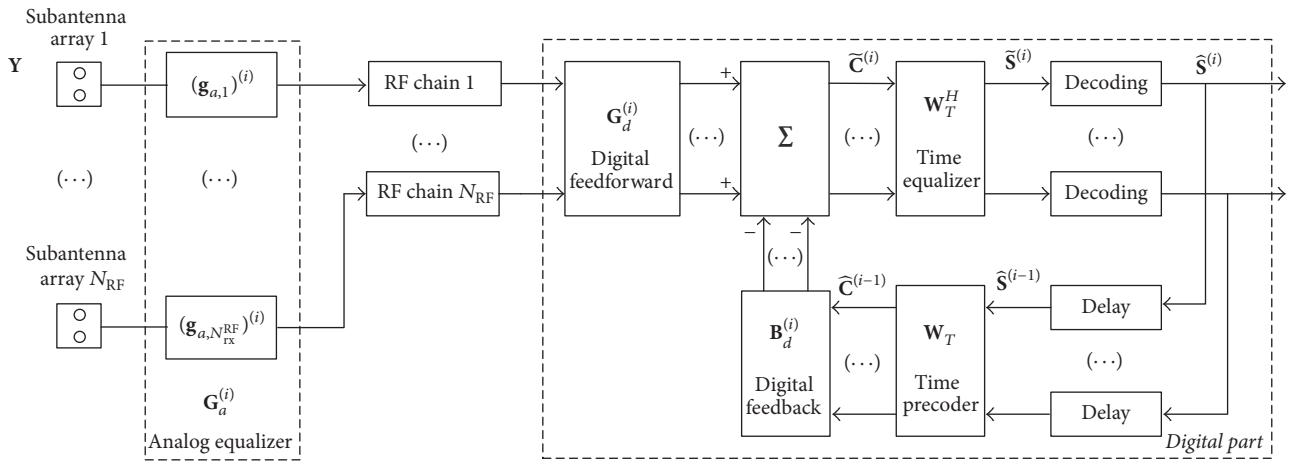

Figure 2: Hybrid iterative multiuser equalizer for subconnected architecture.

selected from a QAM constellation with $\mathbb{E}[|s_{t,u}|^2] = \sigma_u^2$, where $\sum_{u=1}^{U} \sigma_u^2 = U$. The transmitter total power constraint is $\|\mathbf{X}_u\|_F^2 = T$. For the sake of simplicity, and without loss of generality, in this manuscript, only QPSK constellations are considered.

2.3. Receiver Model Description. For a given T-sized block, the received signal is given by

$$\mathbf{y}_t = \sum_{u=1}^{U} \mathbf{H}_u \mathbf{x}_{u,t} + \mathbf{n}_t, \tag{5}$$

where $\mathbf{y}_t \in \mathbb{C}^{N_{\mathrm{rx}}}$ denotes the received signal vector and $\mathbf{n}_t \in \mathbb{C}^{N_{\mathrm{rx}}}$ is the zero mean Gaussian noise vector with variance σ_n^2. This signal is processed at the receiver by an iterative block decoder based in subconnected hybrid architecture, as seen in Figure 2. First, the received signal $\mathbf{y}_t$ is processed through the phase shifters in the analog part, modelled by the vector $\mathbf{g}_{a,p,t} \in \mathbb{C}^R$, where $p \in \{1, \ldots, N_{\mathrm{rx}}^{\mathrm{RF}}\}$ represents the index of the RF chain connected to a set of $R = N_{\mathrm{rx}}/N_{\mathrm{rx}}^{\mathrm{RF}}$ antennas. The global analog matrix $\mathbf{G}_{a,t} \in \mathbb{C}^{N_{\mathrm{rx}}^{\mathrm{RF}} \times N_{\mathrm{rx}}}$ has a block-diagonal structure:

$$\mathbf{G}_{a,t} = \begin{bmatrix} \mathbf{g}_{a,1,t}^T & 0 & 0 & 0 & 0 \\ 0 & \ddots & 0 & 0 & 0 \\ 0 & 0 & \mathbf{g}_{a,p,t}^T & 0 & 0 \\ 0 & 0 & 0 & \ddots & 0 \\ 0 & 0 & 0 & 0 & \mathbf{g}_{a,N_{\mathrm{RF}},t}^T \end{bmatrix}. \tag{6}$$

Baseband processing follows that contains $N_{\mathrm{rx}}^{\mathrm{RF}}$ chains, each one connected to a subset of R antennas, and a closed-loop comprising a digital forward and feedback path. All elements of the vectors $\mathbf{g}_{a,p,t}$ have equal norms ($|\mathbf{g}_{a,p,t}(l)|^2 = N_{\mathrm{rx}}^{-1}$). For the digital forward path, the signal first passes by a linear filter $\mathbf{G}_{d,t} \in \mathbb{C}^{U \times N_{\mathrm{rx}}^{\mathrm{RF}}}$ and then follows a time equalizer and decoding. In the digital feedback path, the recovered data from the forward path first passes through the time precoder and then the feedback matrix $\mathbf{B}_{d,t} = [\mathbf{b}_{d,1,t}, \ldots, \mathbf{b}_{d,U,t}] \in \mathbb{C}^{U \times U}$. The time encoding and decoding of the data symbols obey (4) and

$$\widetilde{\mathbf{S}} = \widetilde{\mathbf{C}} \mathbf{W}_T^H, \tag{7}$$

where the code-word matrix $\widetilde{\mathbf{C}} = [\widetilde{\mathbf{c}}_1, \ldots, \widetilde{\mathbf{c}}_T]$, $\widetilde{\mathbf{c}}_t = [\widetilde{c}_{u,t}]_{1 \le u \le U}$ is a soft estimate of transmitted symbols. Both feedback and feedforward paths are combined; the signal output of the feedback path is subtracted from the filtered received signal $\mathbf{G}_{d,t}\mathbf{G}_{a,t}\mathbf{y}_t$.

This proposed receiver structure is a subconnected hybrid iterative feedback multiuser equalizer, where the main difference from the conventional iterative block decision feedback based equalizers is the analog front-end of constant amplitude phase shifters. The limitation that all elements of each analog vector must have the same norm makes the design of the proposed equalizer harder than for the conventional fully digital one. On the other hand, it assumes a subconnected hybrid architecture, where only a set of antennas is connected to each RF chain, which simplifies the physical implementation when compared with the fully connected hybrid architecture. In the following sections the analog and digital forward matrices, $\mathbf{G}_{a,t}$ and $\mathbf{G}_{d,t}$, are designed, as well as the digital feedback matrix, $\mathbf{B}_{d,t}$.

3. Iterative Receiver Design

In this section, the proposed hybrid iterative multiuser equalizer is derived for subconnected mmWave mMIMO based systems, discussed in the previous section. We assume a decoupled joint transmitter-receiver optimization problem, with the focus on the design of the subconnected hybrid multiuser equalizer.

3.1. MSE Calculation. A block diagram of the proposed iterative multiuser equalizer is shown in Figure 2. The received signal corresponding to user u at the tth time slot for the ith iteration is given by

$$\widetilde{c}_{u,t}^{(i)} = \sum_{p=1}^{N_{\mathrm{rx}}^{\mathrm{RF}}} g_{d,up,t}^{(i)} \left(\mathbf{g}_{a,p,t}^{(i)}\right)^T \mathbf{y}_{p,t} - \left(\mathbf{b}_{d,u,t}^{(i)}\right)^T \widehat{\mathbf{c}}_t^{(i-1)}, \tag{8}$$

where $g_{d,up,t}^{(i)} = \mathbf{G}_{d,t}^{(i)}(u,p)$ is the element of uth row and pth column of $\mathbf{G}_{d,t}^{(i)}$, $\mathbf{g}_{a,p,t}^{(i)} \in \mathbb{C}^R$ denotes the analog part of the feedforward vector of user p, $\mathbf{y}_{p,t} = [\mathbf{y}_t(j)]_{R(p-1)+1\le j\le Rp} \in \mathbb{C}^R$, $\mathbf{b}_{d,u,t}^{(i)} \in \mathbb{C}^U$ is the feedback vector of user u, and $\widehat{\mathbf{c}}_t = [\widehat{c}_{u,t}]_{1\le u\le U} \in \mathbb{C}^U$ is the estimate of the transmitted symbols. The matrix $\widehat{\mathbf{C}}^{(i-1)} = [\widehat{\mathbf{c}}_1^{(i-1)}, \ldots, \widehat{\mathbf{c}}_T^{(i-1)}] \in \mathbb{C}^{U\times T}$ is the DFT of the detector output $\widehat{\mathbf{S}}^{(i-1)}$:

$$\widehat{\mathbf{C}}^{(i-1)} = \widehat{\mathbf{S}}^{(i-1)}\mathbf{W}_T, \tag{9}$$

where $\widehat{\mathbf{S}}^{(i)} = [\widehat{\mathbf{s}}_1, \ldots, \widehat{\mathbf{s}}_t, \ldots, \widehat{\mathbf{s}}_T]$ is the hard decision related to the QPSK data symbols $\mathbf{S} = [\mathbf{s}_1, \ldots, \mathbf{s}_t, \ldots, \mathbf{s}_T]$. At iteration i

$$\widehat{\mathbf{s}}^{(i)} = \mathrm{sign}\left(\widetilde{\mathbf{s}}^{(i)}\right). \tag{10}$$

From the central limit theorem, $\mathbf{c}_t = [c_{u,t}]_{1\le u\le U}$, $u \in \{1,\ldots,U\}$, $t \in \{1,\ldots,T\}$ approximately are Gaussian distributed. In addition, since the input-output relationship between $\mathbf{c}_t$ and $\widehat{\mathbf{c}}_t^{(i)}$, $u \in \{1,\ldots,U\}$, $t \in \{1,\ldots,T\}$ is memoryless, by the Bussgang theorem [38], we have

$$\widehat{\mathbf{c}}_t^{(i)} = \mathbf{\Psi}^{(i)}\mathbf{c}_t + \widehat{\boldsymbol{\epsilon}}_t^{(i)}, \quad t \in \{1,\ldots,T\}, \tag{11}$$

where $\mathbf{\Psi}^{(i)}$ is a diagonal matrix given by

$$\mathbf{\Psi}^{(i)} = \mathrm{diag}\left(\psi_1^{(i)}, \ldots, \psi_u^{(i)}, \ldots, \psi_U^{(i)}\right), \tag{12}$$

$$\psi_u^{(i)} = \frac{\mathbb{E}\left[\widehat{\mathbf{c}}_t^{(i)}(u)\,\mathbf{c}_t^*(u)\right]}{\mathbb{E}\left[\left|\mathbf{c}_t(u)\right|^2\right]}, \quad u \in \{1,\ldots,U\}, \tag{13}$$

and $\widehat{\boldsymbol{\epsilon}}_t^{(i)}$ is an error vector with zero mean and uncorrelated with $\mathbf{c}_t$, $t \in \{1,\ldots,T\}$, with

$$\mathbb{E}\left[\widehat{\boldsymbol{\epsilon}}_t^{(i)}\widehat{\boldsymbol{\epsilon}}_t^{(i)H}\right] = \left(\mathbf{I}_U - \left|\mathbf{\Psi}^{(i)}\right|^2\right)\sigma_u^2. \tag{14}$$

For practical systems, the transmitted signals $\mathbf{c}_t(u)$ are not known a priori and definition (13) cannot be used to compute matrix $\mathbf{\Psi}^{(i)}$, which must be estimated using other methods. Please refer to work [39] where several methods are presented to estimate matrix $\mathbf{\Psi}^{(i)}$.

Define $\mathbf{H}_t = [\mathbf{H}_1\mathbf{f}_{a,1,t}, \ldots, \mathbf{H}_U\mathbf{f}_{a,U,t}] \in \mathbb{C}^{N_{\mathrm{rx}}\times U}$, $\overline{\mathbf{H}}_{p,t} = [\mathbf{H}_t(j,l)]_{R(p-1)+1\le j\le Rp, 1\le l\le U} \in \mathbb{C}^{R\times U}$; therefore, from (8) and (11), it follows that

$$\begin{aligned}\widetilde{c}_{u,t}^{(i)} &= \sum_{p=1}^{N_{\mathrm{rx}}^{\mathrm{RF}}} \left[g_{d,up,t}^{(i)}\left(\mathbf{g}_{a,p,t}^{(i)}\right)^T\left(\overline{\mathbf{H}}_{p,t}\mathbf{c}_t + \mathbf{n}_{p,t}\right)\right] \\ &\quad - \left(\mathbf{b}_{d,u,t}^{(i)}\right)^T\left(\mathbf{\Psi}^{(i-1)}\mathbf{c}_t + \widehat{\boldsymbol{\epsilon}}_t^{(i-1)}\right) \\ &= \sum_{p=1}^{N_{\mathrm{rx}}^{\mathrm{RF}}} \left[g_{d,up,t}^{(i)}\left(\mathbf{g}_{a,p,t}^{(i)}\right)^T\overline{\mathbf{H}}_{p,t}\mathbf{c}_t\right] \\ &\quad + \sum_{p=1}^{N_{\mathrm{rx}}^{\mathrm{RF}}} \left[g_{d,up,t}^{(i)}\left(\mathbf{g}_{a,p,t}^{(i)}\right)^T\mathbf{n}_{p,t}\right] - \left(\mathbf{b}_{d,u,t}^{(i)}\right)^T\mathbf{\Psi}^{(i-1)}\mathbf{c}_t \\ &\quad - \left(\mathbf{b}_{d,u,t}^{(i)}\right)^T\widehat{\boldsymbol{\epsilon}}_t^{(i-1)},\end{aligned} \tag{15}$$

where $\mathbf{n}_{u,t} = [\mathbf{n}_t(j)]_{R(u-1)+1\le j\le Ru} \in \mathbb{C}^R$. Define $\mathbf{g}_{ad,up,t}^{(i)} = g_{d,up,t}^{(i)}\mathbf{g}_{a,p,t}^{(i)} \in \mathbb{C}^R$ and $\widetilde{\epsilon}_{u,t}^{(i)} = \widetilde{c}_{u,t}^{(i)} - c_{u,t}$ which denotes the overall error. Then, by (15), the overall error is

$$\begin{aligned}\widetilde{\epsilon}_{u,t}^{(i)} &= \underbrace{\left(\sum_{p=1}^{N_{\mathrm{rx}}^{\mathrm{RF}}}\left[\left(\mathbf{g}_{ad,up,t}^{(i)}\right)^T\overline{\mathbf{H}}_{p,t}\right] - \left(\mathbf{b}_{d,u,t}^{(i)}\right)^T\mathbf{\Psi}^{(i-1)}\right)\mathbf{c}_t - c_{u,t}}_{\text{Residual ISI}} \\ &\quad - \underbrace{\left(\mathbf{b}_{d,u,t}^{(i)}\right)^T\widehat{\boldsymbol{\epsilon}}_t^{(i-1)}}_{\text{Error from estimate } \widehat{\mathbf{c}}_t^{(i)}} + \underbrace{\sum_{p=1}^{N_{\mathrm{rx}}^{\mathrm{RF}}}\left[\left(\mathbf{g}_{ad,up,t}^{(i)}\right)^T\mathbf{n}_{p,t}\right]}_{\text{Channel Noise}}.\end{aligned} \tag{16}$$

As we can see in (16), the error has three terms: (1) the residual ISI term; (2) the error stemming from the estimate made by $\widehat{\mathbf{c}}_t^{(i)}$ of $c_{u,t}$; and (3) the term corresponding to the channel noise. Let us assume that error $\widetilde{\epsilon}_{u,t}^{(i)}$ is complex Gaussian distributed. From the Bussgang [38] theorem, the zero mean error variable $\widehat{\epsilon}_{u,t}^{(i)}$ is uncorrelated with $c_{u,t}$, and then, from (16), the average error $(\widetilde{\epsilon}_{u,t}^{(i)})$ power, that is, the MSE at time slot t, is given by

$$\begin{aligned}\mathrm{MSE}_{u,t}^{(i)} &= \mathbb{E}\left[\left\|\widetilde{\epsilon}_{u,t}^{(i)}\right\|^2\right] \\ &= \left\|\sum_{p=1}^{N_{\mathrm{rx}}^{\mathrm{RF}}}\left[\left(\mathbf{g}_{ad,up,t}^{(i)}\right)^T\overline{\mathbf{H}}_{p,t}\right] - \mathbf{v}_u^T - \left(\mathbf{b}_{d,u,t}^{(i)}\right)^T\mathbf{\Psi}^{(i-1)}\right\|_F^2\sigma_u^2 \\ &\quad + \left\|\left(\mathbf{b}_{d,u,t}^{(i)}\right)^T\left(\mathbf{I}_U - \left|\mathbf{\Psi}^{(i-1)}\right|^2\right)^{1/2}\right\|_F^2\sigma_u^2 \\ &\quad + \sum_{p=1}^{N_{\mathrm{rx}}^{\mathrm{RF}}}\left\|\left(\mathbf{g}_{ad,up,t}^{(i)}\right)^T\right\|_F^2\sigma_n^2,\end{aligned} \tag{17}$$

where $\mathbf{v}_u = [0,0,\ldots,1,\ldots,0,0]^T \in \mathbb{C}^U$, with the only nonzero value of $\mathbf{v}_u$ in the uth position, and then $c_{u,t} = \mathbf{v}_u^T\mathbf{c}_t$.

3.2. Design of Subconnected Hybrid Iterative Multiuser Equalizer. We start by considering the optimal case, that is, a full digital linear feedforward filter, without the sparsity constraint. We design the iterative multiuser equalizer based on the IB-DFE principles, and we use the average BER as the

metric. The average BER minimization, according to [22], is equivalent to the MSE minimization:

$$\left(\left(\mathbf{g}_{ad,up,t}^{(i)}\right)_{\text{opt}},\left(\mathbf{b}_{d,u,t}^{(i)}\right)_{\text{opt}}\right)=\arg\min \quad \text{MSE}_{u,t}^{(i)} \quad \text{s.t.} \quad \sum_{t=1}^{T}\sum_{p=1}^{N_{\text{rx}}^{\text{RF}}}\left(\mathbf{g}_{ad,up,t}^{(i)}\right)^{T}\overline{\mathbf{H}}_{p,t} = T\mathbf{z}_{U}^{T}, \tag{18}$$

where $\mathbf{g}_{ad,up,t}^{(i)}$ is the linear feedforward filter, $\mathbf{b}_{d,u,t}^{(i)}$ the feedback filter, and $\mathbf{z}_U = [1,1,\ldots,1]^T \in \mathbb{C}^U$ a vector with U ones. The solution to optimization problem (18) is (see the Appendix)

$$\left(\mathbf{g}_{ad,up,t}^{(i)}\right)_{\text{opt}}^{T} = \boldsymbol{\omega}_u\left(\overline{\mathbf{H}}_{p,t}\right)^{H}\left(\mathbf{R}_{p,t}^{(i-1)}\right)^{-1},$$

$$\left(\mathbf{b}_{d,u,t}^{(i)}\right)_{\text{opt}}^{T} = \left(\sum_{p=1}^{N_{\text{rx}}^{\text{RF}}}\left[\left(\mathbf{g}_{ad,up,t}^{(i)}\right)^{T}\overline{\mathbf{H}}_{p,t}\right]-\mathbf{v}_u^{T}\right)\left(\boldsymbol{\Psi}^{(i-1)}\right)^{H},$$

$$\boldsymbol{\omega}_u = T\mathbf{z}_U^{T}\left(\sum_{t=1}^{T}\sum_{p=1}^{N_{\text{rx}}^{\text{RF}}}\left(\overline{\mathbf{H}}_{p,t}\right)^{H}\left(\mathbf{R}_{p,t}^{(i-1)}\right)^{-1}\overline{\mathbf{H}}_{p,t}\right)^{-1},$$

$$\mathbf{R}_{p,t}^{(i-1)} = \left(\overline{\mathbf{H}}_{p,t}\left(\mathbf{I}_U-\left|\boldsymbol{\Psi}^{(i-1)}\right|^2\right)\left(\overline{\mathbf{H}}_{p,t}\right)^{H}+\frac{\sigma_n^2}{\sigma_u^2}\mathbf{I}_R\right). \tag{19}$$

The previous optimization problem of (18) does not reflect the analog domain constraints. Designate $\mathcal{G}_a$ as the set of vectors with constant-magnitude entries, that is, the set of feasible RF equalizers. Thus, the reformulated optimization problem for the subconnected hybrid iterative equalizer is as follows:

$$\left(\left(\mathbf{g}_{a,u,t}^{(i)}\right)_{\text{opt}},\left(g_{d,up,t}^{(i)}\right)_{\text{opt}},\left(\mathbf{b}_{d,u,t}^{(i)}\right)_{\text{opt}}\right)=\arg\min \quad \text{MSE}_{u,t}^{(i)} \quad \text{s.t.} \quad \sum_{t=1}^{T}\sum_{p=1}^{N_{\text{rx}}^{\text{RF}}} g_{d,up,t}^{(i)}\left(\mathbf{g}_{a,p,t}^{(i)}\right)^{T}\overline{\mathbf{H}}_{p,t} = T\mathbf{z}_U^{T}, \quad \mathbf{g}_{a,p,t}^{(i)}\in\mathcal{G}_a,\ p\in\left\{1,\ldots,N_{\text{rx}}^{\text{RF}}\right\}. \tag{20}$$

The feedback equalizer for the subconnected hybrid iterative equalizer is analogous to the fully digital iterative equalizer referred to in the previous section, because the analog domain constraints do not impose any restriction on the vector $\mathbf{b}_{d,u,t}^{(i)}$ and thus are given by

$$\left(\mathbf{b}_{d,u,t}^{(i)}\right)_{\text{opt}}^{T} = \left(\sum_{p=1}^{N_{\text{rx}}^{\text{RF}}}\left[\left(g_{d,up,t}^{(i)}\right)_{\text{opt}}\left(\mathbf{g}_{a,p,t}^{(i)}\right)_{\text{opt}}^{T}\overline{\mathbf{H}}_{p,t}\right]-\mathbf{v}_u^{T}\right)\cdot\left(\boldsymbol{\Psi}^{(i-1)}\right)^{H}. \tag{21}$$

From (17) and (21), the MSE expression is

$$\text{MSE}_{u,t}^{(i)} = \left\|\left(\sum_{p=1}^{N_{\text{rx}}^{\text{RF}}}\left[g_{d,up,t}^{(i)}\left(\mathbf{g}_{a,p,t}^{(i)}\right)^{T}\overline{\mathbf{H}}_{p,t}\right]-\mathbf{v}_u^{T}\right)\times\left(\mathbf{I}_U-\left|\boldsymbol{\Psi}^{(i-1)}\right|^2\right)^{1/2}\right\|_F^2\sigma_u^2 + \sum_{p=1}^{N_{\text{rx}}^{\text{RF}}}\left\|g_{d,up,t}^{(i)}\left(\mathbf{g}_{a,p,t}^{(i)}\right)^{T}\right\|_F^2\sigma_n^2. \tag{22}$$

According to the constraint of (18) $\sum_{p=1}^{N_{\text{rx}}^{\text{RF}}}[(\mathbf{g}_{ad,up,t}^{(i)})_{\text{opt}}^{T}\overline{\mathbf{H}}_{p,t}] = \mathbf{v}_u^{T}$ and therefore (22) can be rewritten as

$$\text{MSE}_{u,t}^{(i)} = \left\|\left(\sum_{p=1}^{N_{\text{rx}}^{\text{RF}}}\left[\left(g_{d,up,t}^{(i)}\left(\mathbf{g}_{a,p,t}^{(i)}\right)^{T}-\left(\mathbf{g}_{ad,up,t}^{(i)}\right)_{\text{opt}}^{T}\right)\overline{\mathbf{H}}_{p,t}\right]\times\left(\mathbf{I}_U-\left|\boldsymbol{\Psi}^{(i-1)}\right|^2\right)^{1/2}\right\|_F^2\sigma_u^2 + \sum_{p=1}^{N_{\text{rx}}^{\text{RF}}}\left\|g_{d,up,t}^{(i)}\left(\mathbf{g}_{a,p,t}^{(i)}\right)^{T}\right\|_F^2\sigma_n^2. \tag{23}$$

Because the feasible set $\mathcal{G}_a$ has a nonconvex nature, an analytical solution to problem (20) is very hard to obtain. However, an approximate solution is possible by assuming that the vector $\mathbf{g}_{a,p,t}^{(i)}$ is a version of vector $\mathbf{a}_{\text{rx},p}(\theta_{j,l}^{\text{rx},p})$. Let $\mathbf{A}_{\text{rx}} = [\mathbf{A}_{\text{rx},1},\ldots,\mathbf{A}_{\text{rx},U}] \in \mathbb{C}^{N_{\text{rx}}\times N_{\text{cl}}N_{\text{ray}}U}$, with $\mathbf{A}_{\text{rx},u} = [\mathbf{a}_{\text{rx},u}(\theta_{1,1}^{\text{rx},u}),\ldots,\mathbf{a}_{\text{rx},u}(\theta_{N_{\text{cl}},N_{\text{ray}}}^{\text{rx},u})] \in \mathbb{C}^{N_{\text{rx}}\times N_{\text{cl}}N_{\text{ray}}}$, forming the matrix with the array response vectors of the receiver, corresponding to user u. As each RF chain is not connected to all antennas, in the selection process of the vector for the pth RF chain, the entries corresponding to the unconnected antennas are removed. For the uth RF chain we use the dictionary $\mathbf{A}_{\text{rx}}^{u} = [\mathbf{A}_{\text{rx}}(j,l)]_{R(u-1)+1\le j\le Ru,1\le l\le N_{\text{cl}}N_{\text{ray}}U} \in \mathbb{C}^{R\times N_{\text{cl}}N_{\text{ray}}U}$, which is a submatrix of $\mathbf{A}_{\text{rx}}$. Then, the vector $\mathbf{g}_{a,u,t}^{(i)}$ is selected from dictionary $\mathbf{A}_{\text{rx}}^{u}$. Therefore, optimization problem (20) can be approximated as follows:

$$\left(\ddot{\mathbf{g}}_{d,up,t}^{(i)}\right)_{\text{opt}} = \arg\min \quad \overline{\text{MSE}}_{u,t}^{(i)}\left(\ddot{\mathbf{g}}_{d,up,t}^{(i)}, \mathbf{A}_{\text{rx}}^{p}\right)$$
$$\text{s.t.} \quad \sum_{t=1}^{T}\sum_{p=1}^{N_{\text{rx}}^{\text{RF}}} \ddot{\mathbf{g}}_{d,up,t}^{(i)}\left(\mathbf{A}_{\text{rx}}^{p}\right)^{H}\overline{\mathbf{H}}_{p,t} = T\mathbf{z}_{U}^{T} \tag{24}$$
$$\left\|\ddot{\mathbf{g}}_{d,up,t}^{(i)}\left(\ddot{\mathbf{g}}_{d,up,t}^{(i)}\right)^{H}\right\|_{0} = 1,$$

where $\ddot{\mathbf{g}}_{d,up,t}^{(i)} = [g_{d,up,t}^{(i)}, \mathbf{0}]^{T} \in \mathbb{C}^{N_{\text{cl}}N_{\text{ray}}U}$ and

$$\overline{\text{MSE}}_{u,t}^{(i)}\left(\ddot{\mathbf{g}}_{d,up,t}^{(i)}, \mathbf{A}_{\text{rx}}^{p}\right) = \left\|\sum_{p=1}^{N_{\text{rx}}^{\text{RF}}}\left[\left(\ddot{\mathbf{g}}_{d,up,t}^{(i)}\left(\mathbf{A}_{\text{rx}}^{p}\right)^{H} - \left(\mathbf{g}_{ad,up,t}^{(i)}\right)_{\text{opt}}\right)\overline{\mathbf{H}}_{p,t}\right]\right.$$
$$\times\left(\mathbf{I}_{U} - \left|\boldsymbol{\Psi}^{(i-1)}\right|^{2}\right)^{1/2}\Bigg\|_{F}^{2}\sigma_{u}^{2} + \sum_{p=1}^{N_{\text{rx}}^{\text{RF}}}\left\|\ddot{\mathbf{g}}_{d,up,t}^{(i)}\left(\mathbf{A}_{\text{rx}}^{p}\right)^{H}\right\|_{F}^{2} \tag{25}$$
$$\cdot\,\sigma_{n}^{2}.$$

The constraint $\|\ddot{\mathbf{g}}_{d,up,t}^{(i)}(\ddot{\mathbf{g}}_{d,up,t}^{(i)})^{H}\|_{0} = 1$ enforces that only one element of vector $\ddot{\mathbf{g}}_{d,up,t}^{(i)}$ is nonzero, representing the sparsity constraint. The optimum digital feedforward vector $(g_{d,up,t}^{(i)})_{\text{opt}}$ is computed from the solution $(\ddot{\mathbf{g}}_{d,up,t}^{(i)})_{\text{opt}}$ of the optimization problem in (24), by removing the zero elements. The optimum analog feedforward vector $(\mathbf{g}_{a,u,t}^{(i)})_{\text{opt}}$ is given by the selected column from $(\mathbf{A}_{\text{rx}}^{u})^{H}$, corresponding to the nonzero element of $\ddot{\mathbf{g}}_{d,up,t}^{(i)}$. Consider optimization problem (24), without the sparsity constraint:

$$\left(\ddot{\mathbf{g}}_{d,u,t}^{(i)}\right)_{\text{opt}} = \arg\min \quad \overline{\text{MSE}}_{u,t}^{(i)}\left(\ddot{\mathbf{g}}_{d,up,t}^{(i)}, \mathbf{A}_{\text{rx}}^{p}\right)$$
$$\text{s.t.} \quad \sum_{t=1}^{T}\sum_{p=1}^{N_{\text{rx}}^{\text{RF}}}\ddot{\mathbf{g}}_{d,up,t}^{(i)}\left(\mathbf{A}_{\text{rx}}^{p}\right)^{H}\overline{\mathbf{H}}_{p,t} = T\mathbf{z}_{U}^{T}. \tag{26}$$

The associated Lagrangian to problem (26) is

$$\mathscr{L}\left(\mu_{u}, \ddot{\mathbf{g}}_{d,up,t}^{(i)}\right) = \overline{\text{MSE}}_{u,t}^{(i)}\left(\ddot{\mathbf{g}}_{d,up,t}^{(i)}, \mathbf{A}_{\text{rx}}^{p}\right) + \mu_{u}\left(\sum_{t=1}^{T}\sum_{p=1}^{N_{\text{rx}}^{\text{RF}}}\ddot{\mathbf{g}}_{d,up,t}^{(i)}\left(\mathbf{A}_{\text{rx}}^{p}\right)^{H}\overline{\mathbf{H}}_{p,t} - T\mathbf{z}_{U}^{T}\right), \tag{27}$$

where $\mu_{u}, u \in \{1, \ldots, U\}$, are the Lagrange multipliers. Taking the derivate in order to obtain $\ddot{\mathbf{g}}_{d,up,t}^{(i)}$, we obtain the optimality condition

$$\frac{\partial\mathscr{L}\left(\mu_{u}, \ddot{\mathbf{g}}_{d,up,t}^{(i)}\right)}{\partial\left(\ddot{\mathbf{g}}_{d,up,t}^{(i)}\right)^{*}} = \mathbf{g}_{\text{res},up,t}^{(i)}\mathbf{A}_{\text{rx}}^{p} = \mathbf{0}, \tag{28}$$

where (28) is the orthogonality principle relative to MSE estimator (24) and $\mathbf{g}_{\text{res},up,t}^{(i)}$ is the residue vector given by

$$\mathbf{g}_{\text{res},up,t}^{(i)} = \left(\ddot{\mathbf{g}}_{d,up,t}^{(i)}\left(\mathbf{A}_{\text{rx}}^{p}\right)^{H} - \left(\mathbf{g}_{ad,up,t}^{(i)}\right)_{\text{opt}}\right)\cdot\overline{\mathbf{H}}_{p,t}\left(\mathbf{I}_{U} - \left|\boldsymbol{\Psi}^{(i-1)}\right|^{2}\right)\left(\overline{\mathbf{H}}_{p,t}\right)^{H} + \ddot{\mathbf{g}}_{d,up,t}^{(i)}\left(\mathbf{A}_{\text{rx}}^{p}\right)^{H}\frac{\sigma_{n}^{2}}{\sigma_{u}^{2}} + \frac{\mu_{u}}{2\sigma_{u}^{2}}\left(\overline{\mathbf{H}}_{p,t}\right)^{H}. \tag{29}$$

An iterative greedy method is used to select the best column of the dictionary $\mathbf{A}_{\text{rx}}^{u}$ allowing enforcement of the sparsity constraint. Due to the mmWave channel nature, the number of the paths is small and, consequently, the complexity of this selection process is low.

Denote $g_{d,up,t}^{(i)}$ and $(\mathbf{g}_{a,u,t}^{(i)})_{\text{opt}}$ as the digital and analog terms of the feedforward vector, corresponding to the selected indices from $\ddot{\mathbf{g}}_{d,up,t}^{(i)}$. For example, if the selected indices are in the first positions, then $\ddot{\mathbf{g}}_{d,up,t}^{(i)} = [g_{d,up,t}^{(i)}, \mathbf{0}]$. Thus, from (29) the orthogonality condition simplifies to

$$\left[\left(g_{d,up,t}^{(i)}\left(\mathbf{g}_{a,p,t}^{(i)}\right)^{T} - \left(\mathbf{g}_{ad,up,t}^{(i)}\right)^{T}\right)\overline{\mathbf{H}}_{p,t}\left(\mathbf{I}_{U} - \left|\boldsymbol{\Psi}^{(i-1)}\right|^{2}\right)\cdot\left(\overline{\mathbf{H}}_{p,t}\right)^{H} + g_{d,up,t}^{(i)}\left(\mathbf{g}_{a,p,t}^{(i)}\right)^{T}\frac{\sigma_{n}^{2}}{\sigma_{u}^{2}} + \frac{\mu_{u}}{2\sigma_{u}^{2}}\left(\overline{\mathbf{H}}_{p,t}\right)^{H}\right]\cdot\left(\mathbf{g}_{a,u,t}^{(i)}\right)^{*} = \mathbf{0}. \tag{30}$$

The solution to (30) is

$$\left(g_{d,up,t}^{(i)}\right)_{\text{opt}} = \boldsymbol{\omega}_{d}\left(\overline{\mathbf{H}}_{p,t}\right)^{H}\left(\mathbf{g}_{a,p,t}^{(i)}\right)^{*} \times\left(\left(\mathbf{g}_{a,p,t}^{(i)}\right)^{T}\mathbf{R}_{p,t}^{(i-1)}\left(\mathbf{g}_{a,p,t}^{(i)}\right)^{*}\right)^{-1}, \tag{31}$$

with $\boldsymbol{\omega}_{d}$, and

$$\boldsymbol{\omega}_{d} = \left(\left(\mathbf{g}_{ad,up,t}^{(i)}\right)^{T}\overline{\mathbf{H}}_{p,t}\left(\mathbf{I}_{U} - \left|\boldsymbol{\Psi}^{(i-1)}\right|^{2}\right) + \frac{\mu_{u}}{2\sigma_{u}^{2}}\right). \tag{32}$$

The Lagrangian multiplier μ_{u} is computed by the power constraint of problem (24), given by

$$\frac{\mu_{u}}{2\sigma_{u}^{2}} = T\mathbf{z}_{U}^{T}\left(\sum_{t=1}^{T}\sum_{p=1}^{N_{\text{rx}}^{\text{RF}}}\left(\overline{\mathbf{H}}_{p,t}\right)^{H}\left(\mathbf{g}_{a,p,t}^{(i)}\right)^{*} \times\left(\left(\mathbf{g}_{a,p,t}^{(i)}\right)^{T}\mathbf{R}_{p,t}^{(i-1)}\left(\mathbf{g}_{a,p,t}^{(i)}\right)^{*}\right)^{-1}\left(\mathbf{g}_{a,p,t}^{(i)}\right)^{T}\overline{\mathbf{H}}_{p,t}\right)^{-1} - \left(\mathbf{g}_{ad,up,t}^{(i)}\right)^{H}\overline{\mathbf{H}}_{p,t}\left(\mathbf{I}_{U} - \left|\boldsymbol{\Psi}^{(i-1)}\right|^{2}\right). \tag{33}$$

After obtaining $g_{d,up,t}^{(i)}$, the optimum value of the digital feedforward part, the previous steps are repeated until

Input: $(\mathbf{g}_{ad,up,t}^{(i)})_{\text{opt}}$

(1) **for** $u \leq N_{\text{rx}}^{\text{RF}}$ **do**

(2) $\mathbf{g}_{\text{res},uu,t}^{(i)} = \left(g_{d,uu,t}^{(i)}\mathbf{g}_{a,u,t}^{(i)} - \left(\mathbf{g}_{ad,uu,t}^{(i)}\right)_{\text{opt}}\right)\overline{\mathbf{H}}_{u,t}\left(\mathbf{I}_U - \left|\boldsymbol{\Psi}^{(i-1)}\right|^2\right)\left(\overline{\mathbf{H}}_{u,t}\right)^H + g_{d,uu,t}^{(i)}\mathbf{g}_{a,u,t}^{(i)}\dfrac{\sigma_n^2}{\sigma_u^2} + \dfrac{\mu_u}{2\sigma_u^2}\left(\overline{\mathbf{H}}_{u,t}\right)^H$

(3) $k = \underset{l=1,\ldots,N_{\text{cl}}N_{\text{ray}}}{\text{argmax}}\left(\left(\mathbf{A}_{\text{rx}}^u\right)^H\left(\mathbf{g}_{\text{res},uu,t}^{(i)}\right)^H\mathbf{g}_{\text{res},uu,t}^{(i)}\left(\mathbf{A}_{\text{rx}}^u\right)\right)_{l,l}$

(4) $\left(\mathbf{g}_{a,u,t}^{(i)}\right)_{\text{opt}} = \left[\left(\left(\mathbf{g}_{a,u,t}^{(i)}\right)_{\text{opt}}\right)^H \mid \left(\mathbf{A}_{\text{rx}}^u\right)^{(k)}\right]^H$

(5) **end for**

(6) $\left(g_{d,up,t}^{(i)}\right)_{\text{opt}} = \boldsymbol{\omega}_d\left(\overline{\mathbf{H}}_{p,t}\right)^H\left(\mathbf{g}_{a,p,t}^{(i)}\right)^H\left(\mathbf{g}_{a,p,t}^{(i)}\mathbf{R}_{p,t}^{(i-1)}\left(\mathbf{g}_{a,p,t}^{(i)}\right)^H\right)^{-1}$

(7) **return** $(\mathbf{g}_{a,u,t}^{(i)})_{\text{opt}}$, $(g_{d,up,t}^{(i)})_{\text{opt}}$

Algorithm 1: The proposed multiuser equalizer for subconnected mmWave massive MIMO architecture.

$u = N_{\text{rx}}^{\text{RF}}$. All steps are synthesized in Algorithm 1, pseudocode of the proposed subconnected hybrid iterative block multiuser equalizer.

4. Performance Results

In this section, we show the performance of the proposed hybrid iterative block multiuser equalizer for subconnected millimeter wave massive MIMO systems. The BER is considered the performance metric, presented as a function of E_b/N_0, where E_b is the average bit energy and N_0 is the one-sided noise power spectral density. The power of each UT is normalized to $\sigma_1^2 = \cdots = \sigma_U^2 = 1$ and the channel matrix, as previously mentioned, is normalized, such that $\mathbb{E}[\|\mathbf{H}_u\|_F^2] = N_{\text{rx}}N_{\text{tx}}$. Then, the average E_b/N_0 for all users $u \in \{1,\ldots,U\}$ is identical and given by $E_b/N_0 = \sigma_u^2/(2\sigma_n^2) = \sigma_n^{-2}/2$.

The carrier frequency was set to 72 GHz and was considered a clustered narrowband channel model [40] for each user with $N_{\text{cl}} = 8$ clusters, all with the same average power, and $N_{\text{ray}} = 4$ rays per cluster. The azimuth angles of arrival and departure of the channel model are Laplacian distributed as in [21]. We assumed an angle spread equal to 8° at both the transmitter and receiver and uniform linear arrays (ULAs) with antenna element spacing equal to half-wavelength; however, the subconnected hybrid equalizer developed in this paper can be applied to any antenna arrays. The channel remains constant during a block with size T but varies independently between them. We assume perfect synchronization and CSI knowledge at the receiver side. All results were obtained for a QPSK modulation. We present results for two main scenarios, all with $N_{\text{tx}} = 8$. The other parameters are as follows.

Scenario 1 ($U = N_{\text{rx}}^{\text{RF}} = 8$).

(1.a) $N_{\text{rx}} = 16$ ($R = 2$).

(1.b) $N_{\text{rx}} = 32$ ($R = 4$).

(1.c) $N_{\text{rx}} = 48$ ($R = 6$).

Scenario 2 ($U = N_{\text{rx}}^{\text{RF}} = 4$).

(2.a) $N_{\text{rx}} = 8$ ($R = 2$).

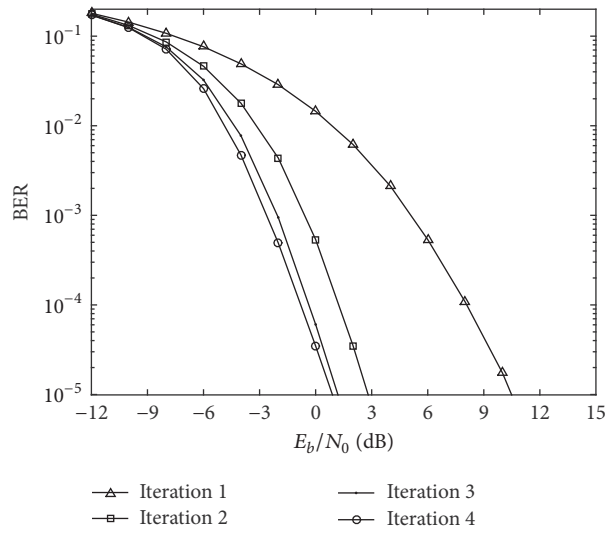

Figure 3: Performance of the proposed subconnected hybrid multiuser equalizer for scenario (1.b).

(2.b) $N_{\text{rx}} = 16$ ($R = 4$).

(2.c) $N_{\text{rx}} = 24$ ($R = 6$).

Here $R = N_{\text{rx}}/N_{\text{rx}}^{\text{RF}}$ represents the number of antennas per RF chain. In both scenarios, we assume the full load case (worst case), where the number of users and RF chains is equal. To compute the proposed subconnected hybrid equalizer, we consider that $\mathbf{f}_{a,u,t}$, the analog precoder for the uth user, is generated according to (2). As mentioned before, the motivation is to keep the UTs with very low complexity without the knowledge of CSI before transmission. The proposed subconnected hybrid iterative multiuser equalizer is referred to here as *subconnected*. The results are compared with both fully digital, referred to here as *digital,* and fully connected, referred to as *fully connected*, which was recently proposed in [22], approaches.

Start with the results obtained for scenario (1.b) presented in Figures 3 and 4. In Figure 3, we present results for iterations 1, 2, 3, and 4 of the proposed subconnected hybrid iterative

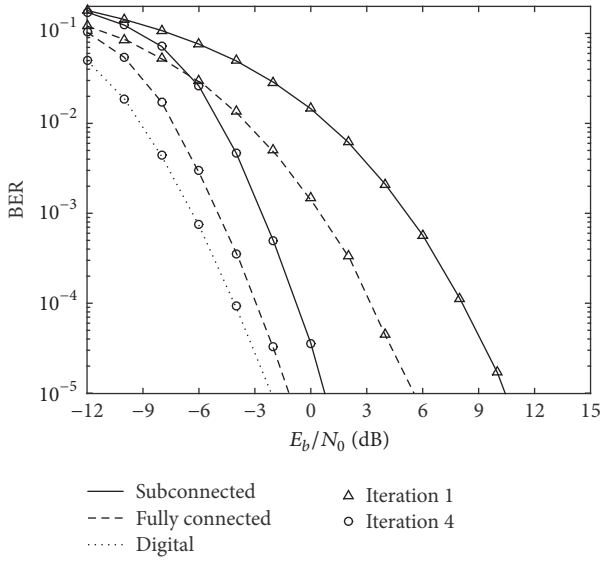

Figure 4: Performance comparison of the proposed subconnected hybrid multiuser equalizer with a fully connected approach for scenario (1.b).

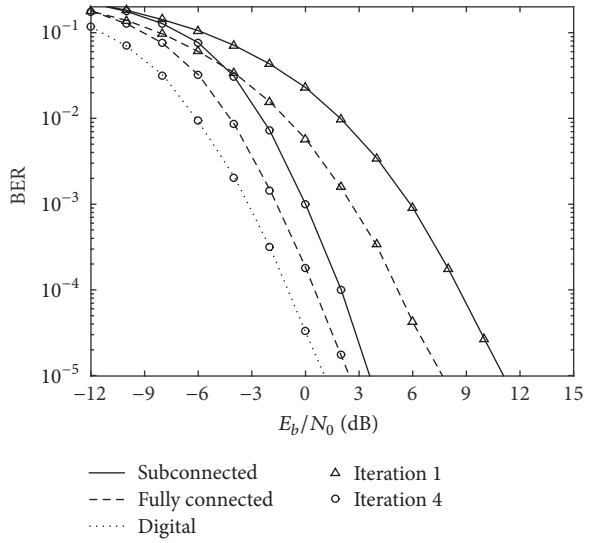

Figure 5: Performance comparison of the proposed subconnected hybrid multiuser equalizer with a fully connected approach for scenario (2.b).

multiuser equalizer. It can be seen that the performance improves as the number of iterations increases, as expected. Additionally, the gaps between the 1st and 2nd iterations are much higher than between the 3rd and 4th iterations. This occurs because most of the residual intersymbol and multiuser interferences are removed from the 1st to the 2nd iteration. For this scenario, the results with the fully digital and fully connected hybrid multiuser equalizer are presented in Figure 4. In this figure, we verify that the *subconnected* performance is worse than both *digital* and *fully connected* approaches, mainly for the first iteration. However, for the 4th iteration we can see that the performance of the proposed subconnected hybrid multiuser equalizer is close to the *digital* and *fully connected* counterparts. Therefore, we can argue that the dictionary approximation and the sequential optimization are quite precise.

Compare scenario (1.b) with scenario (2.b) presented in Figure 5, where the number of users and RF chains ($U = N_{\text{rx}}^{\text{RF}}$) changes, but the number of antennas per RF chain is the same; that is, $R = 4$. In scenario (1.b), at a target BER of 10^{-3}, the penalties of the proposed subconnected equalizer for the *fully connected* and *digital* approaches are 2.3 dB and 3.8 dB, respectively, at the 4th iteration. In scenario (2.b), for the same target BER and iteration, the penalties for *fully connected* and *digital* are approximately 1.6 dB and 3.2 dB, slightly decreasing for lower $U = N_{\text{rx}}^{\text{RF}}$. We can also see that for scenario (1.b) a lower E_b/N_0 is needed to achieve a BER of 10^{-5} compared with scenario (2.b). This is because scenario (1.b) can achieve higher diversity and array gain given by the larger dimension of the receiving antenna array. When we reduce the number of antennas per RF chain by half, that is, for $R = 2$, which corresponds to scenario (1.a) presented in Figure 6, we verify that the penalty for *fully connected* and *digital* approaches is approximately 1.2 dB and

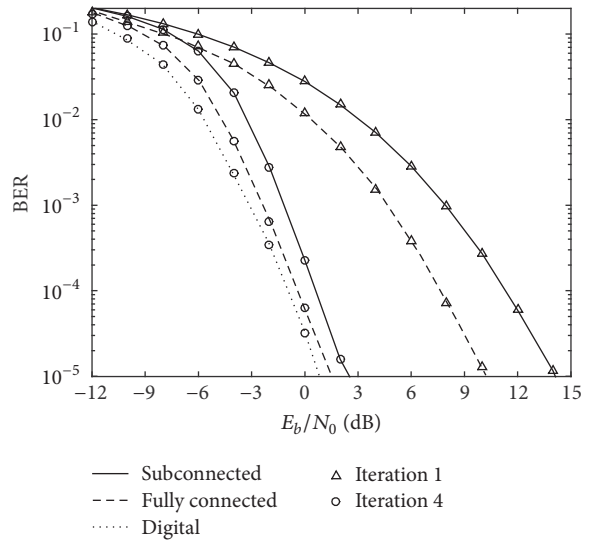

Figure 6: Performance comparison of the proposed subconnected hybrid multiuser equalizer with a fully connected approach for scenario (1.a).

1.9 dB, thus decreasing for lower R. This occurs because when we reduce R, the subconnected architecture tends toward the fully digital case. In the extreme case where $R = 1$, we have one antenna per RF chain, that is, the digital architecture. As expected, by reducing R the degrees of freedom of the subconnected architecture increase, and the gap with the *fully connected* and *digital* approaches decreases. For the digital equalizer the curve for iteration 1 is not presented in Figures 4, 5, and 6 to improve the intelligibility since it almost overlaps with the curve for iteration 4 of the proposed scheme.

In Figures 7 and 8, we compare the performance of the *subconnected* approach for Scenarios 1 and 2 by considering

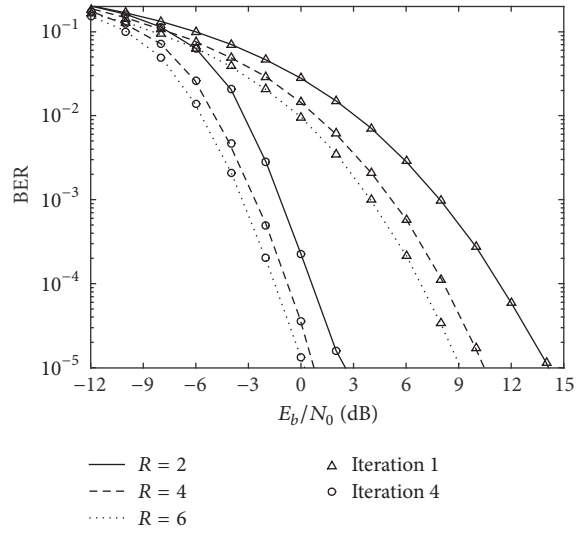

Figure 7: Performance comparison of the proposed subconnected hybrid multiuser equalizer for $R = 2, 4$, and 6, for Scenario 1.

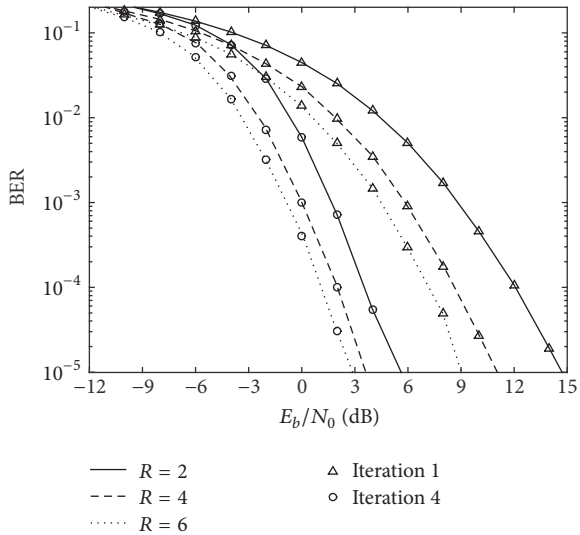

Figure 8: Performance comparison of the proposed subconnected hybrid multiuser equalizer for $R = 2, 4$, and 6, for Scenario 2.

$R = 2, 4$, and 6 antennas per RF chain. Although the penalty of the proposed subconnected multiuser equalizer relative to the *fully connected* and *digital* increases with R, as previously verified, the BER performance of the subconnected multiuser equalizer improves with R because the diversity and antenna gain are higher due to a larger number of receiving antennas.

Notably, the above was considered the worst case, where $U = N_{\text{rx}}^{\text{RF}}$. Improved BER performance would be achieved for $U < N_{\text{rx}}^{\text{RF}}$, that is, for a number of users (streams) lower than the number of RF chains. For that case, the performance gaps between the proposed subconnected hybrid multiuser equalizer and the *digital*/*fully connected* approaches would be even smaller.

5. Conclusions

We designed a new hybrid iterative multiuser equalizer for a subconnected mmWave massive MIMO architecture. We considered low complexity UTs employing randomly analog-only precoding and a single RF chain. First, it was verified that the proposed hybrid iterative multiuser equalizer converges and that it achieves a performance close to the *digital* and *fully connected* counterparts, requiring very few iterations. This structure efficiently manages multiuser interference; the dictionary approximation and the sequential optimization are quite precise. We observed that when we reduce the number of receiving antennas per RF chain, that is, $R = N_{\text{rx}}/N_{\text{rx}}^{\text{RF}}$, the BER performance gets worse due to the reduction of both the antenna gain and diversity. We also observed that the gap between the proposed *subconnected*scheme and the *digital*/*fully connected* approaches decreases when R decreases, because the architecture becomes closer to the *digital* one.

The performance of the proposed receiver structure shows that it is interesting for practical mmWave massive MIMO based systems, that is, the systems where hardware constraints are considered. This means that the number of transmit/receiving RF chains is much lower than the number of transmit/receiving antennas, and each RF chain is only connected to a reduced number of antennas, ensuring good performance at a low cost.

Appendix

Solution for Optimization Problem (18)

The Lagrangian associated with problem (18) is

$$\begin{aligned}
&\mathscr{L}\left(\mu_u, \mathbf{g}_{ad,up,t}^{(i)}, \mathbf{b}_{d,u,t}^{(i)}\right) \\
&\quad = \left\| \sum_{p=1}^{N_{\text{rx}}^{\text{RF}}} \left[\left(\mathbf{g}_{ad,up,t}^{(i)}\right)^T \overline{\mathbf{H}}_{p,t} \right] - \mathbf{v}_u^T - \left(\mathbf{b}_{d,u,t}^{(i)}\right)^T \boldsymbol{\Psi}^{(i-1)} \right\|_F^2 \\
&\quad \cdot \sigma_u^2 + \left\| \left(\mathbf{b}_{d,u,t}^{(i)}\right)^T \left(\mathbf{I}_U - \left| \boldsymbol{\Psi}^{(i-1)} \right|^2 \right)^{1/2} \right\|_F^2 \sigma_u^2 \\
&\quad + \sum_{p=1}^{N_{\text{rx}}^{\text{RF}}} \left\| \left(\mathbf{g}_{ad,up,t}^{(i)}\right)^T \right\|_F^2 \sigma_n^2 \\
&\quad + \mu_u \left(\sum_{t=1}^{T} \sum_{p=1}^{N_{\text{rx}}^{\text{RF}}} \left(\mathbf{g}_{ad,up,t}^{(i)}\right)^T \overline{\mathbf{H}}_{p,t} - T\mathbf{z}_U \right),
\end{aligned} \tag{A.1}$$

where $\mu_u, u \in \{1, \ldots, U\}$, are the Lagrange multipliers. For the optimization variable $(\mathbf{b}_{d,u,t}^{(i)})^T$, the correspondent first-order optimality condition [41, 42] is

$$\begin{aligned}
&\frac{\mathscr{L}\left(\mu_u, \mathbf{g}_{ad,up,t}^{(i)}, \mathbf{b}_{d,u,t}^{(i)}\right)}{\partial \left(\left(\mathbf{b}_{d,u,t}^{(i)}\right)^T \right)^*} \\
&\quad = 2 \left(\mathbf{b}_{d,u,t}^{(i)}\right)^T \sigma_u^2
\end{aligned}$$

$$-2\left(\sum_{p=1}^{N_{\mathrm{rx}}^{\mathrm{RF}}}\left[\left(\mathbf{g}_{ad,up,t}^{(i)}\right)^{T}\overline{\mathbf{H}}_{p,t}\right]-\mathbf{v}_{u}^{T}\right)\left(\boldsymbol{\Psi}^{(i-1)}\right)^{H}\sigma_{u}^{2}=\mathbf{0}, \tag{A.2}$$

whose solution gives the optimum value of $(\mathbf{b}_{d,u,t}^{(i)})^{T}$:

$$\left(\mathbf{b}_{d,u,t}^{(i)}\right)_{\mathrm{opt}}^{T}=\left(\sum_{p=1}^{N_{\mathrm{rx}}^{\mathrm{RF}}}\left[\left(\mathbf{g}_{ad,up,t}^{(i)}\right)^{T}\overline{\mathbf{H}}_{p,t}\right]-\mathbf{v}_{u}^{T}\right)\left(\boldsymbol{\Psi}^{(i-1)}\right)^{H}. \tag{A.3}$$

From (A.3), the Lagrangian function simplifies to

$$\begin{aligned}\mathscr{L}\left(\mu_{u},\mathbf{g}_{ad,up,t}^{(i)}\right)=&\left\|\left(\sum_{p=1}^{N_{\mathrm{rx}}^{\mathrm{RF}}}\left[\left(\mathbf{g}_{ad,up,t}^{(i)}\right)^{T}\overline{\mathbf{H}}_{p,t}\right]-\mathbf{v}_{u}^{T}\right)\right.\\&\left.\cdot\left(\mathbf{I}_{U}-\left|\boldsymbol{\Psi}^{(i-1)}\right|^{2}\right)^{1/2}\right\|_{F}^{2}\sigma_{u}^{2}+\sum_{p=1}^{N_{\mathrm{rx}}^{\mathrm{RF}}}\left\|\left(\mathbf{g}_{ad,up,t}^{(i)}\right)^{T}\right\|_{F}^{2}\sigma_{n}^{2}\\&+\mu_{u}\left(\sum_{t=1}^{T}\sum_{p=1}^{N_{\mathrm{rx}}^{\mathrm{RF}}}\left(\mathbf{g}_{ad,up,t}^{(i)}\right)^{T}\overline{\mathbf{H}}_{p,t}-T\mathbf{I}_{U}\right).\end{aligned} \tag{A.4}$$

By taking the derivate in relation to $(\mathbf{g}_{ad,up,t}^{(i)})^{T}$

$$\begin{aligned}\frac{\mathscr{L}\left(\mu_{u},\mathbf{g}_{ad,up,t}^{(i)}\right)}{\partial\left(\left(\mathbf{g}_{ad,up,t}^{(i)}\right)^{T}\right)^{*}}=&2\left(\left(\mathbf{g}_{ad,up,t}^{(i)}\right)^{T}\overline{\mathbf{H}}_{p,t}-\mathbf{v}_{u}^{T}\right)\\&\cdot\left(\mathbf{I}_{U}-\left|\boldsymbol{\Psi}^{(i-1)}\right|^{2}\right)\left(\overline{\mathbf{H}}_{p,t}\right)^{H}\sigma_{u}^{2}\\&+2\left(\mathbf{g}_{ad,up,t}^{(i)}\right)^{T}\sigma_{n}^{2}+\mu_{u}\left(\overline{\mathbf{H}}_{p,t}\right)^{H},\end{aligned} \tag{A.5}$$

and setting it equal to zero, we obtain

$$\begin{aligned}\left(\mathbf{g}_{ad,up,t}^{(i)}\right)_{\mathrm{opt}}^{T}=&\left(\mathbf{v}_{u}^{T}\left(\mathbf{I}_{U}-\left|\boldsymbol{\Psi}^{(i-1)}\right|^{2}\right)-\frac{\mu_{u}}{2\sigma_{u}^{2}}\right)\left(\overline{\mathbf{H}}_{p,t}\right)^{H}\\&\times\left(\overline{\mathbf{H}}_{p,t}\left(\mathbf{I}_{U}-\left|\boldsymbol{\Psi}^{(i-1)}\right|^{2}\right)\left(\overline{\mathbf{H}}_{p,t}\right)^{H}+\frac{\sigma_{n}^{2}}{\sigma_{u}^{2}}\mathbf{I}_{R}\right)^{-1}.\end{aligned} \tag{A.6}$$

The Lagrangian multipliers μ_u may be redefined to $\boldsymbol{\omega}_u = \mathbf{v}_u(\mathbf{I}_U - |\boldsymbol{\Psi}^{(i-1)}|^2) - 0.5\sigma_u^{-2}\mu_u$. By considering

$$\mathbf{R}_{p,t}^{(i-1)}=\left(\overline{\mathbf{H}}_{p,t}\left(\mathbf{I}_{U}-\left|\boldsymbol{\Psi}^{(i-1)}\right|^{2}\right)\left(\overline{\mathbf{H}}_{p,t}\right)^{H}+\frac{\sigma_{n}^{2}}{\sigma_{u}^{2}}\mathbf{I}_{R}\right) \tag{A.7}$$

(A.6) then reduces to

$$\left(\mathbf{g}_{ad,up,t}^{(i)}\right)_{\mathrm{opt}}^{T}=\boldsymbol{\omega}_{u}\left(\overline{\mathbf{H}}_{p,t}\right)^{H}\left(\mathbf{R}_{p,t}^{(i-1)}\right)^{-1}. \tag{A.8}$$

The optimum feedforward vector $(\mathbf{g}_{ad,up,t}^{(i)})_{\mathrm{opt}}$ must respect the constraint of problem (18). From (A.8) and the constraint of problem (18), we find that

$$\begin{aligned}&\sum_{t=1}^{T}\sum_{p=1}^{N_{\mathrm{rx}}^{\mathrm{RF}}}\boldsymbol{\omega}_{u}\left(\overline{\mathbf{H}}_{p,t}\right)^{H}\left(\mathbf{R}_{p,t}^{(i-1)}\right)^{-1}\overline{\mathbf{H}}_{p,t}\\&=\boldsymbol{\omega}_{u}\sum_{t=1}^{T}\sum_{p=1}^{N_{\mathrm{rx}}^{\mathrm{RF}}}\left(\overline{\mathbf{H}}_{p,t}\right)^{H}\left(\mathbf{R}_{p,t}^{(i-1)}\right)^{-1}\overline{\mathbf{H}}_{p,t}=T\mathbf{z}_{U}.\end{aligned} \tag{A.9}$$

Thus, $\boldsymbol{\omega}_u$ is given by

$$\boldsymbol{\omega}_{u}=T\mathbf{z}_{U}^{T}\left(\sum_{t=1}^{T}\sum_{p=1}^{N_{\mathrm{rx}}^{\mathrm{RF}}}\left(\overline{\mathbf{H}}_{p,t}\right)^{H}\left(\mathbf{R}_{p,t}^{(i-1)}\right)^{-1}\overline{\mathbf{H}}_{p,t}\right)^{-1}. \tag{A.10}$$

Conflicts of Interest

The authors declare that they have no conflicts of interest.

Acknowledgments

This work is funded by Instituto de Telecomunicações (IT) and Fundação para a Ciência e a Tecnologia (FCT) through project PURE-5GNET (UID/EEA/50008/2013).

References

[1] T. E. Bogale and L. B. Le, "Massive MIMO and mmWave for 5G wireless HetNet: potential benefits and challenges," *IEEE Vehicular Technology Magazine*, vol. 11, no. 1, pp. 64–75, 2016.

[2] K. N. R. S. V. Prasad, E. Hossain, and V. K. Bhargava, "Energy efficiency in massive mimo-based 5G networks: opportunities and challenges," *IEEE Wireless Communications Magazine*, 2017.

[3] M. Agiwal, A. Roy, and N. Saxena, "Next generation 5G wireless networks: a comprehensive survey," *IEEE Communications Surveys & Tutorials*, vol. 18, no. 3, pp. 1617–1655, 2016.

[4] A. Gupta and R. K. Jha, "A survey of 5G network: architecture and emerging technologies," *IEEE Access*, vol. 3, pp. 1206–1232, 2015.

[5] K. Zheng, L. Zhao, J. Mei, B. Shao, W. Xiang, and L. Hanzo, "Survey of large-scale MIMO systems," *IEEE Communications Surveys & Tutorials*, vol. 17, no. 3, pp. 1738–1760, 2015.

[6] Z. Gao, L. Dai, D. Mi, Z. Wang, M. A. Imran, and M. Z. Shakir, "MmWave massive-MIMO-based wireless backhaul for the 5G ultra-dense network," *IEEE Wireless Communications Magazine*, vol. 22, no. 5, pp. 13–21, 2015.

[7] L. Lu, G. Y. Li, A. L. Swindlehurst, A. Ashikhmin, and R. Zhang, "An overview of massive MIMO: benefits and challenges," *IEEE Journal of Selected Topics in Signal Processing*, vol. 8, no. 5, pp. 742–758, 2014.

[8] T. E. Bogale and L. B. Le, "Beamforming for multiuser massive MIMO systems: digital versus hybrid analog-digital," in *Proceedings of the IEEE Global Communications Conference (GLOBECOM '14)*, pp. 4066–4071, Austin, Tex, USA, December 2014.

[9] T. E. Bogale, L. B. Le, A. Haghighat, and L. Vandendorpe, "On the number of RF chains and phase shifters, and scheduling

design with hybrid analog-digital beamforming," *IEEE Transactions on Wireless Communications*, vol. 15, no. 5, pp. 3311–3326, 2016.

[10] E. W. Jang, J. Lee, H.-L. Lou, and J. M. Cioffi, "On the combining schemes for MIMO systems with hybrid ARQ," *IEEE Transactions on Wireless Communications*, vol. 8, no. 2, pp. 836–842, 2009.

[11] C.-X. Wang, F. Haider, X. Gao et al., "Cellular architecture and key technologies for 5G wireless communication networks," *IEEE Communications Magazine*, vol. 52, no. 2, pp. 122–130, 2014.

[12] J. G. Andrews, S. Buzzi, and W. Choi, "What will 5G be?" *IEEE Journal on Selected Areas in Communications*, vol. 32, no. 6, pp. 1065–1082, 2014.

[13] J. Wang, Z. Lan, C.-W. Pyo et al., "Beam codebook based beamforming protocol for multi-Gbps millimeter-wave WPAN systems," *IEEE Journal on Selected Areas in Communications*, vol. 27, no. 8, pp. 1390–1399, 2009.

[14] O. E. Ayach, R. W. Heath Jr., S. Abu-Surra, S. Rajagopal, and Z. Pi, "The capacity optimality of beam steering in large millimeter wave MIMO systems," in *Proceedings of the 2012 IEEE 13th International Workshop on Signal Processing Advances in Wireless Communications, SPAWC 2012*, pp. 100–104, 2012.

[15] A. Alkhateeb, J. Mo, N. González-Prelcic, and R. W. Heath Jr., "MIMO precoding and combining solutions for millimeter-wave systems," *IEEE Communications Magazine*, vol. 52, no. 12, pp. 122–131, 2014.

[16] H. Shuangfeng, I. Chih-Lin, X. Zhikun, and C. Rowell, "Large-scale antenna systems with hybrid analog and digital beamforming for millimeter wave 5G," *IEEE Communications Magazine*, vol. 53, no. 1, pp. 186–194, 2015.

[17] O. E. Ayach, S. Rajagopal, S. Abu-Surra, Z. Pi, and R. W. Heath, "Spatially sparse precoding in millimeter wave MIMO systems," *IEEE Transactions on Wireless Communications*, vol. 13, no. 3, pp. 1499–1513, 2014.

[18] X. Gao, L. Dai, C. Yuen, and Z. Wang, "Turbo-like beamforming based on tabu search algorithm for millimeter-wave massive mimo systems," *IEEE Transactions on Vehicular Technology*, vol. 65, no. 7, pp. 5731–5737, 2016.

[19] Z. Xiao, T. He, P. Xia, and X.-G. Xia, "Hierarchical codebook design for beamforming training in millimeter-wave communication," *IEEE Transactions on Wireless Communications*, vol. 15, no. 5, pp. 3380–3392, 2016.

[20] J. Li, L. Xiao, X. Xu, and S. Zhou, "Robust and low complexity hybrid beamforming for uplink multiuser MmWave MIMO Systems," *IEEE Communications Letters*, vol. 20, no. 6, pp. 1140–1143, 2016.

[21] A. Alkhateeb, G. Leus, and R. W. Heath, "Limited feedback hybrid precoding for multi-user millimeter wave systems," *IEEE Transactions on Wireless Communications*, vol. 14, no. 11, pp. 6481–6494, 2015.

[22] R. Magueta, D. Castanheira, A. Silva, R. Dinis, and A. Gameiro, "Hybrid iterative space-time equalization for multi-user mmW massive MIMO systems," *IEEE Transactions on Communications*, vol. 65, no. 2, pp. 608–620, 2017.

[23] N. Benvenuto, R. Dinis, D. Falconer, and S. Tomasin, "Single carrier modulation with nonlinear frequency domain equalization: an idea whose time has come—again," *Proceedings of the IEEE*, vol. 98, no. 1, pp. 69–96, 2010.

[24] N. Benvenuto and S. Tomasin, "Block iterative DFE for single carrier modulation," *IEEE Electronics Letters*, vol. 38, no. 19, pp. 1144-1145, 2002.

[25] Y.-C. Liang, S. Sun, and C. K. Ho, "Block-iterative generalized decision feedback equalizers for large MIMO systems: algorithm design and asymptotic performance analysis," *IEEE Transactions on Signal Processing*, vol. 54, no. 6, pp. 2035–2048, 2006.

[26] R. Kalbasi, D. D. Falconer, A. H. Banihashemi, and R. Dinis, "A comparison of frequency-domain block MIMO transmission systems," *IEEE Transactions on Vehicular Technology*, vol. 58, no. 1, pp. 165–175, 2009.

[27] M. Luzio, R. Dinis, and P. Montezuma, "SC-FDE for offset modulations: an efficient transmission technique for broadband wireless systems," *IEEE Transactions on Communications*, vol. 60, no. 7, pp. 1851–1861, 2012.

[28] P. Li and R. C. De Lamare, "Adaptive decision-feedback detection with constellation constraints for MIMO systems," *IEEE Transactions on Vehicular Technology*, vol. 61, no. 2, pp. 853–859, 2012.

[29] A. Silva, S. Teodoro, R. Dinis, and A. Gameiro, "Iterative frequency-domain detection for IA-precoded MC-CDMA systems," *IEEE Transactions on Communications*, vol. 62, no. 4, pp. 1240–1248, 2014.

[30] D. Castanheira, A. Silva, R. Dinis, and A. Gameiro, "Efficient transmitter and receiver designs for SC-FDMA based heterogeneous networks," *IEEE Transactions on Communications*, vol. 63, no. 7, pp. 2500–2510, 2015.

[31] S. Mumtaz, J. Rodriguez, and L. Dai, *mmWave Massive MIMO: A Paradigm for 5G*, Academic Press, 1st edition, 2016.

[32] S. Park, A. Alkhateeb, and R. W. Heath, "Dynamic subarray architecture for wideband hybrid precoding in millimeter wave massive MIMO systems," in *Proceedings of the 2016 IEEE Global Conference on Signal and Information Processing (GlobalSIP)*, pp. 600–604, Washington DC, USA, December 2016.

[33] L. He, J. Wang, and J. Song, "Spatial modulation for more spatial multiplexing: RF-chain-limited generalized spatial modulation aided MmWave MIMO with hybrid precoding Scheme," 2017, https://arxiv.org/abs/1704.08824v1.

[34] S. He, C. Qi, Y. Wu, and Y. Huang, "Energy-efficient transceiver design for hybrid sub-array architecture MIMO systems," *IEEE Access*, vol. 4, pp. 9895–9905, 2016.

[35] F. Sohrabi and W. Yu, "Hybrid analog and digital beamforming for OFDM-based large-scale MIMO systems," in *Proceedings of the 17th IEEE International Workshop on Signal Processing Advances in Wireless Communications, SPAWC 2016*, July 2016.

[36] X. Gao, L. Dai, S. Han, I. Chih-Lin, and R. W. Heath, "Energy-efficient hybrid analog and digital precoding for MmWave MIMO systems with large antenna arrays," *IEEE Journal on Selected Areas in Communications*, vol. 34, no. 4, pp. 998–1009, 2016.

[37] A. Li and C. Masouros, "Hybrid analog-digital millimeter-wave MU-MIMO transmission with virtual path selection," *IEEE Communications Letters*, vol. 21, no. 2, pp. 438–441, 2017.

[38] H. E. Rowe, "Memoryless nonlinearities with gaussian inputs: elementary results," *Bell System Technical Journal*, vol. 61, no. 7, pp. 1519–1526, 1982.

[39] F. Silva, R. Dinis, and P. Montezuma, "Estimation of the feedback reliability for IB-DFE receivers," *ISRN Communications and Networking*, vol. 2011, Article ID 980830, pp. 980830-7, 2011.

[40] M. R. Akdeniz, Y. Liu, M. K. Samimi et al., "Millimeter wave channel modeling and cellular capacity evaluation," *IEEE Journal on Selected Areas in Communications*, vol. 32, no. 6, pp. 1164–1179, 2014.

[41] R. T. Rockafellar, *Convex Analysis*, Princeton University Press, Princeton, NJ, USA, 1997.

[42] S. Boyd and L. Vandenberghe, *Convex Optimization*, Cambridge University Press, Cambridge, UK, 2004.